Inorg. Chem. **2009**, *48*, 307−318

Radical Formation in the [$MeReO_3$]-Catalyzed Aqueous Peroxidative Oxidation of Alkanes: A Theoretical Mechanistic Study

Maxim L. Kuznetsov and Armando J. L. Pombeiro*

Centro de Química Estrutural, Complexo I, Instituto Superior Técnico, TU Lisbon, Av. Rovisco Pais, 1049-001 Lisbon, Portugal

Received September 12, 2008

Plausible mechanisms of radical formation in the catalytic system [$MeReO_3$]/H_2O_2/H_2O−CH_3CN for the oxidation of alkanes to alcohols and ketones, via radical pathways, are investigated extensively at the density functional theory level. The most favorable route is based on the monoperoxo complex [$MeReO_2(O_2)(H_2O)$] and includes the formation of an H_2O_2 adduct, water-assisted H-transfer from H_2O_2 to the peroxo ligand, and generation of HOO•. The thus formed reduced Re^{VI} complex [$MeReO_2(OOH)(H_2O)$] reacts with H_2O_2, resulting, upon water-assisted H-transfer and O−OH bond homolysis, in the regeneration of the oxo−Re^{VII} catalyst and formation of the HO• radical that reacts further with the alkane. Water plays a crucial role by (i) stabilizing transition states for the proton migrations and providing easy intramolecular H-transfers in the absence of any *N*,*O*-ligands and (ii) saturating the Re coordination sphere what leads to a decrease of the activation barrier for the formation of HOO•. The activation energy of the radical formation calculated for [$MeReO_3$] (17.7 kcal/mol) is compatible with that determined experimentally [Shul'pin et al. *J. Chem. Soc., Perkin Trans. 2* **2001**, 1351.] for oxo−V-based catalytic systems (17 ± 2 kcal/mol), and the overall type of mechanism proposed for such V catalysts is also effective for [$MeReO_3$].

Introduction

Saturated hydrocarbons (alkanes) are the most abundant and cheapest carbon raw materials, and their functionalization leading to industrially valuable products currently attracts great attention.[1−3] They can be oxidized to the corresponding alcohols and/or ketones in processes catalyzed by some metal complexes and metal oxides,[3−7] e.g., oxides of V,[8−11] Mo,[12] Re,[13] Cu,[14] Ru,[15−17] or Os.[18]One of the most effective and environmentally friendly oxidants (or promotor of the oxidation) in these reactions is hydrogen peroxide.[8,9,10b−e,h,13,14] A free-radical mechanism of such alkane oxidations catalyzed by some oxo−vanadium (V) species containing *N*,*O*-ligands in the presence of H_2O_2 was proposed by Shul'pin et al.,[9] and the first part of such a mechanism, i.e., the free radical generation, was recently studied theoretically by Bell

* To whom correspondence should be addressed. E-mail: pombeiro@ist.utl.pt.

(1) (a) Derouane, E. G.; Parmon, F.; Lemos, F.; Ramôa Ribeiro, F. (Eds). *Sustainable Strategies for the Upgrading of Natural Gas: Fundamentals, Challenges, and Opportunities*; NATO Science Series, vol. 191, Kluwer Academic: Dordrecht, 2005. (b) Shilov, A. E.; Shul'pin, G. B. *Activation and Catalytic Reactions of Saturated Hydrocarbons in the Presence of Metal Complexes*; Kluwer Academic: Dordrecht, 2000. (c) Hill, C. L. *Activation and Functionalization of Alkanes*; Wiley: New York, 1989.
(2) Crabtree, R. H. *J. Chem. Soc., Dalton Trans.* **2001**, 2437.
(3) Shilov, A. E.; Shul'pin, G. B. *Chem. Rev.* **1997**, *97*, 2879.
(4) Shul'pin, G. B. C. R. *Chimie* **2003**, *6*, 163.
(5) Shul'pin, G. B. *J. Mol. Catal. A* **2002**, *189*, 39.
(6) Schuchardt, U.; Cardoso, D.; Sercheli, R.; Pereira, R.; da Cruz, R. S.; Guerreiro, M. C.; Mandelli, D.; Spinacé, E. V.; Pires, E. L. *Appl. Catal., A* **2001**, *211*, 1.
(7) Brégeault, J.-M. *Dalton Trans.* **2003**, 3289.
(8) (a) Reis, P. M.; Silva, J. A. L.; Fraústo da Silva, J. J. R.; Pombeiro, A. J. L. *Chem. Commun.* **2000**, 1845. (b) Shul'pin, G. B.; Mishra, G. S.; Shul'pina, L. S.; Strelkova, T. V.; Pombeiro, A. J. L. *Catal. Commun.* **2007**, *8*, 1516. (c) Mishra, G. S.; Fraústo da Silva, J. J. R.; Pombeiro, A. J. L. *J. Mol. Catal. A* **2007**, *265*, 59.
(9) (a) Shul'pin, G. B.; Kozlov, Y. N.; Nizova, G. V.; Süss-Fink, G.; Stanislas, S.; Kitaygorodskiy, A.; Kulikova, V. S. *J. Chem. Soc., Perkin Trans. 2* **2001**, 1351. (b) Kozlov, Y. N.; Romakh, V. B.; Kitaygorodskiy, A.; Buglyó, P.; Süss-Fink, G.; Shul'pin, G. B. *J. Phys. Chem. A* **2007**, *111*, 7736.
(10) (a) Shul'pin, G. B.; Nizova, G. V. *React. Kinet. Catal. Lett.* **1991**, *45*, 7. (b) Shil'pin, G. B.; Guerreiro, M. C.; Schuchardt, U. *Tetrahedron* **1996**, *52*, 13051. (c) Nizova, G. V.; Süss-Fink, G.; Shul'pin, G. B. *Tetrahedron* **1997**, *53*, 3603. (d) Süss-Fink, G.; Nizova, G. V.; Stanislas, S.; Shul'pin, G. B. *J. Mol. Catal. A* **1998**, *130*, 163. (e) de la Cruz, M. H. C.; Kozlov, Y. N.; Lachter, E. R.; Shul'pin, G. B. *New. J. Chem.* **2003**, *27*, 634. (f) Shul'pin, G. B.; Lachter, E. R. *J. Mol. Catal. A* **2003**, *197*, 65. (g) Cuervo, L. G.; Kozlov, Y. N.; Süss-Fink, G.; Shul'pin, G. B. *J. Mol. Catal. A* **2004**, *218*, 171. (h) Kozlov, Y. N.; Nizova, G. V.; Shul'pin, G. B. *J. Mol. Catal. A* **2005**, *227*, 247.
(11) (a) Teramura, K.; Tanaka, T.; Hosokawa, T.; Ohuchi, T.; Kani, M.; Funabiki, T. *Catal. Today* **2004**, *96*, 205. (b) Teramura, K.; Tanaka, T.; Kani, M.; Hosokawa, T.; Funabiki, T. *J. Mol. Catal. A* **2004**, *208*, 299.

10.1021/ic801753t CCC: $40.75
Published on Web 12/02/2008

Scheme 1. Simplified Catalytic Cycle for the V-Assisted Formation of HOO• and HO• Radicals Proposed by Shul'pin et al.[9]

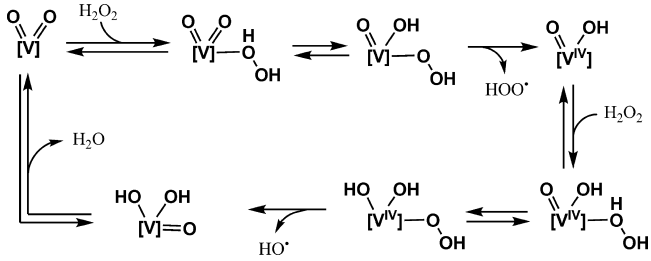

et al.[19] This mechanism involves the formation of an adduct of the catalyst with an H_2O_2 molecule followed by H-transfer to the oxo ligand and elimination of hydroperoxyl (HOO•) to yield a V^{IV} species (Scheme 1). Then hydroxyl (HO•) radical may be formed as a result of the reaction of H_2O_2 with this V^{IV} complex, and it reacts with the alkane (RH) to produce, by H-abstraction, the corresponding alkyl radical (R•), which undergoes further transformations.

However, for many of the above-mentioned catalytic systems, the reached conversion is rather low and the usage of additives (cocatalysts), high temperature, or photoirradiation is necessary. Some V complexes, such as amavadine and its models, being among the best catalysts for these processes,[8] are not easily accessible due to the complexity of their synthesis. Recently,[20] one of us has reported that an efficient single-pot oxidation of liquid alkanes, e.g. cyclopentane and cyclohexane, to the corresponding alcohols and ketones may be achieved under mild conditions (room temperature, aqueous H_2O_2, in the absence of any additives) using some commercially available group 5−7 metal oxides as catalysts, e.g., rhenium oxides including methyltrioxorhenium(VII) [$MeReO_3$] (MTO, **1**).

MTO is a very effective catalyst for a number of reactions,[21,22] among them alkane oxidation;[13c,20] epoxidation of olefins; oxidations of aromatic compounds,[13c,21,23,24] alkynes,[25] sulfur compounds,[26] phosphines, arsines, stibines,[27] amines,[28] alcohols,[29] ketones,[30] and halide ions;[31] the corresponding deoxygenation processes;[32] aldehyde olefination;[33] olefin metathesis;[34] and activation of hydrogen peroxide.[35] However, the application of MTO for catalytic alkane oxidations is still very limited,[13,20] and the mechanism of these reactions and the role of MTO as catalyst have not yet been studied.

Our recent experimental results[20] indicate that the alkane oxidations in the system [$MeReO_3$]/H_2O_2/H_2O−CH_3CN proceed via generation of both O- and C-centered free radicals. It was found that the catalytic activity was greatly inhibited or even suppressed in the presence of an O- or C-centered radical trap, such as Ph_2NH, $CBrCl_3$, 2,2,6,6-tetramethylpiperidine-1-oxyl (TEMPO), or 2,6-di-*tert*-butyl-4-methylphenol (BHT). In such a situation, a Shul'pin's type mechanism[9] can be considered as a reasonable starting proposal. This hypothesis had not yet been explored for MTO-catalyzed alkane oxidations, although there is a number of theoretical works devoted to the analysis of other mechanisms and the role of MTO in different reactions, e.g., olefin epoxidation.[23,24d,36] Thus, the main goals of the present work are (i) to investigate in detail, using density functional theory, the possible pathways (and to establish the most plausible ones) of the radical formation (the first and rate-limiting stage of the Shul'pin's vanadium mechanism) in the system [$MeReO_3$]/H_2O_2/H_2O−CH_3CN and (ii) to broaden the application of such a type of mechanisms

(12) Liu, H.-F.; Liu, R.-S.; Liew, K. Y.; Johnson, R. E.; Lunsford, J. H. *J. Am. Chem. Soc.* **1984**, *106*, 4117.
(13) (a) Alegria, E. C. B.; Kirillova, M. V.; Martins, L. M. D. R. S.; Pombeiro, A. J. L. *Appl. Catal., A* **2007**, *317*, 43. (b) Murray, R. W.; Iyanar, K.; Chen, J.; Wearing, J. T. *Tetrahedron Lett.* **1995**, *36*, 6415. (c) Schuchardt, U.; Mandelli, D.; Shul'pin, G. B. *Tetrahedron Lett.* **1996**, *37*, 6487.
(14) (a) Kirillov, A. M.; Kopylovich, M. N.; Kirillova, M. V.; Haukka, M.; Guedes da Silva, M. F. C.; Pombeiro, A. J. L. *Angew. Chem., Int. Ed.* **2005**, *44*, 4345. (b) Kirillov, A. M.; Kopylovich, M. N.; Kirillova, M. V.; Karabach, E. Y.; Haukka, M.; Guedes da Silva, M. F. C.; Pombeiro, A. J. L. *Adv. Synth. Catal.* **2006**, *348*, 159.
(15) Tenaglia, A.; Terranova, E.; Waegell, B. *J. Chem. Soc., Chem. Commun.* **1990**, 1344.
(16) (a) Bakke, J. M.; Frøhaug, A. E. *J. Phys. Org. Chem.* **1996**, *9*, 310.
(17) Bakke, J. M.; Frøhaug, A. E. *J. Phys. Org. Chem.* **1996**, *9*, 507.
(18) (a) Bales, B. C.; Brown, P.; Dehestani, A.; Mayer, J. M. *J. Am. Chem. Soc.* **2005**, *127*, 2832. (b) Shul'pin, G. B.; Süss-Fink, G.; Shul'pina, L. S. *Chem. Commun.* **2000**, 1131. (c) Shul'pin, G. B.; Kudinov, A. R.; Shul'pina, L. S.; Petrovskaya, E. A. *J. Organomet. Chem.* **2006**, *691*, 837.
(19) Khaliullin, R. Z.; Bell, A. T.; Head-Gordon, M. *J. Phys. Chem. B* **2005**, *109*, 17984.
(20) Kirillova, M. V.; Kirillov, A. M.; Reis, P. M.; Silva, J. A. L.; Fraústo da Silva, J. J. R.; Pombeiro, A. J. L. *J. Catal.* **2007**, *248*, 130.
(21) Herrmann, W. A.; Kühn, F. E. *Acc. Chem. Res.* **1997**, *30*, 169, and references herein.
(22) (a) Kühn, F. E.; Santos, A. M.; Herrmann, W. A. *Dalton Trans.* **2005**, 2483. (b) Kühn, F. E.; Scherbaum, A.; Herrmann, W. A. *J. Organomet. Chem.* **2004**, *689*, 4149. (c) Herrmann, W. A. *J. Organomet. Chem.* **1995**, *500*, 149.
(23) Deubel, D. V.; Frenking, G.; Gisdakis, P.; Herrmann, W. A.; Rösch, N.; Sundermeyer, J. *Acc. Chem. Res.* **2004**, *37*, 645.
(24) (a) Herrmann, W. A.; Fischer, R. W.; Marz, D. W. *Angew. Chem., Int. Ed. Engl.* **1991**, *30*, 1638. (b) Herrmann, W. A.; Fischer, R. W.; Rauch, M. U.; Scherer, W. *J. Mol. Catal.* **1994**, *86*, 243. (c) Rudolph, J.; Reddy, K. L.; Chiang, J. P.; Sharpless, K. B. *J. Am. Chem. Soc.* **1997**, *119*, 6189. (d) Kühn, F. E.; Santos, A. M.; Roesky, P. W.; Herdtweck, E.; Scherer, W.; Gisdakis, P.; Yudanov, I. V.; Valentin, C. D.; Rösch, N. *Chem. Eur. J.* **1999**, *5*, 3603. (e) Adam, W.; Mitchell, C. M.; Saha-Möller, C. R. *J. Org. Chem.* **1999**, *64*, 3699.
(25) Zhu, Z.; Espenson, J. H. *J. Org. Chem.* **1995**, *60*, 7728.
(26) (a) Huston, P.; Espenson, J. H.; Bakac, A. *Inorg. Chem.* **1993**, *32*, 4517. (b) Vassell, K. A.; Espenson, J. H. *Inorg. Chem.* **1994**, *33*, 5491. (c) Adam, W.; Mitchell, C. M.; Saha-Möller, C. R. *Tetrahedron* **1994**, *50*, 13121. (d) Lahti, D. W.; Espenson, J. H. *Inorg. Chem.* **2000**, *39*, 2164.
(27) Abu-Omar, M. M.; Espenson, J. H. *J. Am. Chem. Soc.* **1995**, *117*, 272.
(28) (a) Zhu, Z.; Espenson, J. H. *J. Org. Chem.* **1995**, *60*, 1326. (b) Murray, R. W.; Iyanar, K.; Chen, J.; Wearing, J. T. *Tetrahedron Lett.* **1996**, *37*, 805.
(29) Zauche, T. H.; Espenson, J. H. *Inorg. Chem.* **1998**, *37*, 6827.
(30) Abu-Omar, M. M.; Espenson, J. H. *Organometallics* **1996**, *15*, 3543.
(31) (a) Espenson, J. H.; Pestovsky, O.; Huston, P.; Staudt, S. *J. Am. Chem. Soc.* **1994**, *116*, 2869. (b) Hansen, P. J.; Espenson, J. H. *Inorg. Chem.* **1995**, *34*, 5389.
(32) Zhu, Z.; Espenson, J. H. *J. Mol. Catal. A* **1995**, *103*, 87.
(33) Herrmann, W. A.; Wang, M. *Angew. Chem., Int. Ed. Engl.* **1991**, *30*, 1641.
(34) (a) Verkuijlen, E.; Kapsteijn, F.; Mol, J. C.; Boelhouwer, C. *J. Chem. Soc., Chem. Commun.* **1977**, 198. (b) Moulijn, J. A.; Boelhouwer, C. *J. Chem. Soc., Chem. Commun.* **1979**, 330. (c) Herrmann, W. A.; Wagner, W.; Flessner, U. N.; Volkhardt, U.; Komber, H. *Angew. Chem., Int. Ed. Engl.* **1991**, *30*, 1636.
(35) Espenson, J. H. *Chem. Commun.* **1999**, 479.
(36) (a) Gisdakis, P.; Antonczak, S.; Köstlmeier, S.; Herrmann, W. A.; Rösch, N. *Angew. Chem., Int. Ed.* **1998**, *37*, 2211. (b) Gisdakis, P.; Yudanov, I. V.; Rösch, N. *Inorg. Chem.* **2001**, *40*, 3755. (c) Valentin, C. D.; Gandolfi, R.; Gisdakis, P.; Rösch, N. *J. Am. Chem. Soc.* **2001**, *123*, 2365.

(initially proposed for a particular oxo−vanadium catalyst) to an oxo−rhenium system with a different composition, thus attempting to widen its scope. Additionally, equilibria in solution containing MTO, H_2O_2, and water have been investigated in detail.

Computational Details

The full geometry optimization of all structures and transition states has been carried out at the DFT level of theory using Becke's three-parameter hybrid exchange functional in combination with the gradient-corrected correlation functional of Lee, Yang, and Parr (B3LYP)[37] with the help of the Gaussian 98[38] program package. Restricted approximations for the structures with closed electron shells and the unrestricted methods for the structures with open electron shells have been employed. Symmetry operations were not applied for all structures. The geometry optimization was carried out using a quasirelativistic Stuttgart pseudopotential that described 60 core electrons and the appropriate contracted basis set (8s7p6d)/[6s5p3d][39] for the rhenium atom and the 6-31G(d) basis set for other atoms. Then, for the species involved in the discussed mechanisms, single-point calculations were performed on the basis of the found equilibrium geometries using the 6-311G(d,p) basis set for nonmetal atoms. Test calculations indicated that the full geometry optimization at the B3LYP/6-311G(d,p) level gives relative energies and structural parameters that are very similar to those obtained at the B3LYP/6-311G(d,p)//B3LYP/6-31G(d) level. The addition of a f-type exponent on Re also did not result in noticeable change of the relative energies and structural parameters.

The Hessian matrix was calculated analytically for the optimized structures at the B3LYP/6-31G(d) level in order to prove the location of correct minima (no "imaginary" frequencies) or saddle points (only one negative eigenvalue) and to estimate the thermodynamic parameters, the latter being calculated at 25 °C. The nature of all transition states was investigated by the analysis of vectors associated with the "imaginary" frequency.

Total energies corrected for solvent effects (E_s) were estimated at the single-point calculations on the basis of gas-phase geometries at the CPCM-B3LYP/6-311G(d,p)//gas-B3LYP/6-31G(d) level of theory using the polarizable continuum model in the CPCM version[40] with CH_3CN and, in some cases, H_2O as solvents. The entropic term in CH_3CN solution (S_s) was calculated according to the procedure described by Wertz[41] and Cooper and Ziegler[42] using eqs 1−4

$$\Delta S_1 = R \ln V^{s}_{m,liq}/V_{m,gas} \quad (1)$$

$$\Delta S_2 = R \ln V^{\circ}_{m}/V^{s}_{m,liq} \quad (2)$$

$$\alpha = \frac{S^{\circ,s}_{liq} - (S^{\circ,s}_{gas} + R \ln V^{s}_{m,liq}/V_{m,gas})}{(S^{\circ,s}_{gas} + R \ln V^{s}_{m,liq}/V_{m,gas})} \quad (3)$$

$$S_s = S_g + \Delta S_{sol} = S_g + [\Delta S_1 + \alpha(S_g + \Delta S_1) + \Delta S_2] = S_g + [(-12.21 \text{ cal/mol K}) - 0.23(S_g - 12.21 \text{ cal/mol K}) + 5.87 \text{ cal/mol K}] \quad (4)$$

where S_g is the gas-phase entropy of solute, ΔS_{sol} is the solvation entropy, $S^{\circ,s}_{liq}$, $S^{\circ,s}_{gas}$, and $V^{s}_{m,liq}$ are the standard entropies and molar volume of the solvent in liquid or gas phases (149.62 J/mol K, 245.48 J/mol K, and 52.16 mL/mol, respectively, for CH_3CN), $V_{m,gas}$ is the molar volume of the ideal gas at 25 °C (24 450 mL/mol), and V°_{m} is the molar volume of the solution corresponding to the standard conditions (1000 mL/mol). The enthalpies and Gibbs free energies in solution (H_s and G_s) were estimated using expressions 5 and 6

$$H_s = E_s(\text{6-311(d,p)}) + H_g(\text{6-31G(d)}) - E_g(\text{6-31G(d)}) \quad (5)$$

$$G_s = H_s - T\Delta S_s \quad (6)$$

where E_s, E_g, and H_g are the total energies in solution and in gas phase and the gas-phase enthalpy calculated at the corresponding level.

For some complexes with long metal−ligand bonds, the topological analysis of the electron density distribution with help of the AIM method of Bader[43] was determined using the programs GRIDV, GRDVEC, CONTOR, and EXT94B.[44]

Results and Discussion

On the basis of experimental[35,45] and theoretical[36a,b] studies, it was shown that in solution, in the presence of hydrogen peroxide, MTO undergoes peroxidation to afford mono- and diperoxo complexes that are in equilibrium with the initial MTO (Scheme 2). Hence, we shall consider plausible mechanisms based on these three forms of the catalyst, i.e. MTO and mono- and diperoxo complexes. The majority of the complexes described in the present paper have several possible isomers, and the most stable isomeric forms are indicated by index "a" following the number of the corresponding complex. The less stable isomers are marked by other letters ("b", "c", etc.) in the order of the decreasing stability. The general view of the equilibrium structures and total energies for all the calculated isomers are given in the Supporting Information (Table 1S). In the text, only the most plausible pathways are discussed, whereas less favorable routes, along with complete versions of schemes and tables illustrating the reaction mechanisms, are deposited as Supporting Information.

(37) (a) Becke, A. D. *J. Chem. Phys.* **1993**, *98*, 5648. (b) Lee, C.; Yang, W.; Parr, R. G. *Phys. Rev.* **1988**, *B37*, 785.
(38) Frisch, M. J. ; Trucks, G. W.; Schlegel, H. B.; Scuseria, G. E.; Robb, M. A.; Cheeseman, J. R.; Zakrzewski, V. G.; Montgomery, J. A., Jr.; Stratmann, R. E.; Burant, J. C.; Dapprich, S.; Millam, J. M.; Daniels, A. D.; Kudin, K. N.; Strain, M. C.; Farkas, O.; Tomasi, J.; Barone, V.; Cossi, M.; Cammi, R.; Mennucci, B.; Pomelli, C.; Adamo, C.; Clifford, S.; Ochterski, J.; Peterson, G. A.; Ayala, P. Y.; Cui, Q.; Morokuma, K.; Malick, D. K.; Rabuck, A. D.; Raghavachari, K.; Foresman, J. B.; Cioslowski, J.; Ortiz, J. V.; Baboul, A. G.; Stefanov, B. B.; Liu, G.; Liashenko, A.; Piskorz, P.; Komaromi, I.; Gomperts, R.; Martin, R. L.; Fox, D. J.; Keith, T.; Al-Laham, M. A.; Peng, C. Y.; Nanayakkara, A.; Challacombe, M.; Gill, P. M. W.; Johnson, B.; Chen, W.; Wong, M. W.; Andres, J. L.; Gonzalez, C.; Head-Gordon, M.; Replogle, E. S.; Pople, J. A. *Gaussian 98, revision A.9*; Gaussian, Inc.: Pittsburgh, PA, 1998.
(39) Andrae, D.; Haeussermann, U.; Dolg, M.; Stoll, H.; Preuss, H. *Theor. Chim. Acta* **1990**, *77*, 123.
(40) (a) Tomasi, J.; Persico, M. *Chem. Rev.* **1997**, *94*, 2027. (b) Barone, V.; Cossi, M. *J. Phys. Chem.* **1998**, *102*, 1995.
(41) Wertz, D. H. *J. Am. Chem. Soc.* **1980**, *102*, 5316.
(42) Cooper, J.; Ziegler, T. *Inorg. Chem.* **2002**, *41*, 6614.
(43) Bader, R. F. W. *Atoms in Molecules: A Quantum Theory*; Oxford University Press: Oxford, 1990.
(44) Biegler-König, F. W.; Bader, R. F. W.; Tang, T.-H. *J. Comput. Chem.* **1982**, *3*, 317.
(45) (a) Herrmann, W. A.; Fischer, R. W.; Scherer, W.; Rauch, M. U. *Angew. Chem., Int. Ed. Engl.* **1993**, *32*, 1157. (b) Abu-Omar, M. M.; Hansen, P. J.; Espenson, J. H. *J. Am. Chem. Soc.* **1996**, *118*, 4966.

Scheme 2. Equilibria in the $[MeReO_3]/H_2O_2/H_2O$ System (L, L′ = H_2O, H_2O_2)

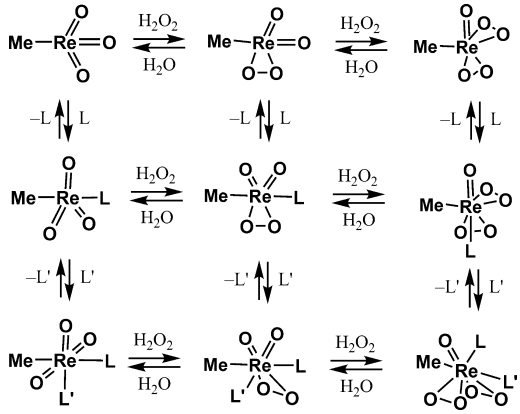

1. Mechanisms Based on $[MeReO_3]$. (i) Initial Adducts. In solution, the MTO molecule can interact with other species bearing donor atoms, e.g. solvents (H_2O, CH_3CN) and H_2O_2, leading to penta- or hexa-coordinate complexes. Our calculations demonstrate that formation of the adducts of MTO with acetonitrile and hydrogen peroxide, i.e., $[MeReO_3L]$ [L = CH_3CN (**2**), H_2O_2 (**3**)] [Schemes 3 and 1S (Supporting Information)]—the H_2O_2 complex corresponding to the proposed starting V species in Shul'pin's mechanism (Scheme 1)—is slightly (by 2.5−3.7 kcal/mol) endoergonic (Scheme 3B, Table 1; the complete version of Table 1 is given in Supporting Information as Table 2S). The water adduct **4** lies 0.5 kcal/mol lower in energy[46] than the corresponding starting reactants. No transition states for these processes were found, and complexes **2**−**4** are formed without overcoming of a potential barrier. This and also the fact that the structure of the $MeReO_3$ core changes insignificantly from **1** to **2**−**4** indicate that the adducts should be considered as orientation molecular complexes with a weakened Re−O_L bond rather than a complex with a "normal" Re−O_L donor−acceptor bond, and the L ligands may be easily liberated or interchanged. Each of the complexes **3** and **4** has two stable isomers with similar energies (Table 1S, Supporting Information), and the geometry of one of them (**3b** and **4a**) as well as that of **2** correspond to experimental X-ray structures for complexes of the type $[MeReO_3(OR)]$, e.g., $[MeReO_3(ONC_5H_4\text{-}^tBu)]$.[47] For **2**, only one stable isomer was found, and its energy of formation is higher than those of **3** and **4**. The general mechanism of radical formation may also include hexa-coordinate Re complexes with a saturated coordination sphere, e.g., the aqua−peroxo adduct $[MeReO_3(H_2O)(H_2O_2)]$ (**5**) for which only one stable isomer was found.

(ii) Proton Migration. The next step of a plausible mechanism is an intramolecular H-transfer from the bound H_2O_2 to an oxo-ligand in complexes **3** or **5** affording the corresponding hydroxo−hydroperoxo species $[MeReO_2(OH)(OOH)]$ **6** or $[MeReO_2(OH)(OOH)(H_2O)]$ **7** [the most stable isomers **6a** and **7a**, Schemes 3 and 1S (Supporting Information)]. On the basis of experimental kinetic studies,[48] it was proposed that this type of reaction proceeds via formation of a four-membered cyclic transition state. However, although our calculations allowed the location of transition states (TSs) of such a type ($\mathbf{TS_{3a-6a}}$ and $\mathbf{TS_{5-7a}}$, Figures 1a and 2), the estimated activation enthalpy (20.9 and 23.8 kcal/mol, Table 1) is significantly higher than that obtained[48] experimentally (6.9 ± 0.4 kcal/mol).

It was shown[9,19] that for the similar process in vanadium complexes bearing an *N*,*O*-ligand {e.g., $[VO_2(H_2O_2)(pca)]$, pca = deprotonated form of pyrazine-2-carboxylic acid}, this ligand plays a key role in the H-shift from H_2O_2 to the oxo ligand. In the proposed "robot's arm" mechanism, the H-transfer occurs first to the *N*,*O*-ligand with the cleavage of a metal−ligand bond and only then to the oxo ligand. As a result, the activation energy for the overall process is 4.3 kcal/mol lower compared to the direct H-transfer from H_2O_2 to the oxo ligand.[19]

The rhenium complexes **3** and **5** do not contain any *N*,*O*- or other ligands that may be involved into a stepwise H-transfer. However, considering that the reaction occurs in the presence of water, the TSs may include an additional H_2O molecule from the outer sphere ($\mathbf{TS_{3a-6a,H_2O}}$ and $\mathbf{TS_{5-7a,H_2O}}$, Figures 1b and 2). These TSs bear a six-membered metallacycle (b) that is more stable than the four-membered cycle (a) involved in the direct H-shift from the ligated H_2O_2 to an oxo ligand. The activation barriers for such water-assisted reactions are much smaller ($\Delta H_s^{\ddagger}$ are 6.8 and 8.8 kcal/mol for water solution, in perfect agreement with the experiment, and 2.5 and 2.7 kcal/mol for acetonitrile solution).

(iii) Radical formation. Complexes **6** and **7** are the species which, in principle, may directly produce hydroperoxyl ($HOO^{\bullet}$) radicals. These radicals may be generated (Scheme 3) either as a result of simple homolytic cleavage of the M−OOH bond in **6** or **7** {**6** → $[MeReO_2(OH)]$ **8** + $HOO^{\bullet}$ or **7** → $[MeReO_2(OH)(H_2O)]$ **9** + $HOO^{\bullet}$} (S_N1 process) or as a result of S_N2 substitution of the OOH ligand with H_2O in **6** or **7** {**6** → **9** or **7** → $[MeReO_2(OH)(H_2O)_2]$ **10**}. However, despite the extensive search for the potential energy surface (PES), we were unable to locate any transition state for the concerted one-step S_N2 substitutions.

The calculated enthalpies for the S_N1 generation of $HOO^{\bullet}$ radicals from **6a** and **7a** (that is, the adiabatic M−OOH bond enthalpies) are 31.8 and 25.9 kcal/mol, respectively (Table 1). The latter value is even lower than the corresponding energy calculated[19] for the $HOO^{\bullet}$ radical liberation from the hydroperoxo−vanadium complex $[V(OO)(OOH)_2(pca)]$ (30 kcal/mol).

The ΔH_s value of formation of **8** + $HOO^{\bullet}$ relative to the level of the initial compounds **1** and H_2O_2 (i.e., apparent activation enthalpy, $\Delta H_{s,ap}$) is 28.1 kcal/mol (Table 1, Scheme 3B), which is significantly higher than the apparent activation energy obtained experimentally[9] and theoretically[19] for the similar process involving the oxo−vanadium catalysts (15−19

(46) Herein and onwards, if not stated otherwise, the ΔG_s difference is given for the relative stabilities and activation barriers. See the section Computational Details for the estimate of G_s.

(47) Herrmann, W. A.; Correia, J. D. G.; Rauch, M. U.; Artus, J. R. G.; Kuhn, F. E. *J. Mol. Catal. A* **1997**, *118*, 33.

(48) Pestovsky, O.; van Eldik, R.; Huston, P.; Espenson, J. H. *J. Chem. Soc., Dalton Trans.* **1995**, 133.

Scheme 3. Mechanisms of HOO• Formation Based on [$MeReO_3$] (A) and the Corresponding Energy Profile (B)[a]

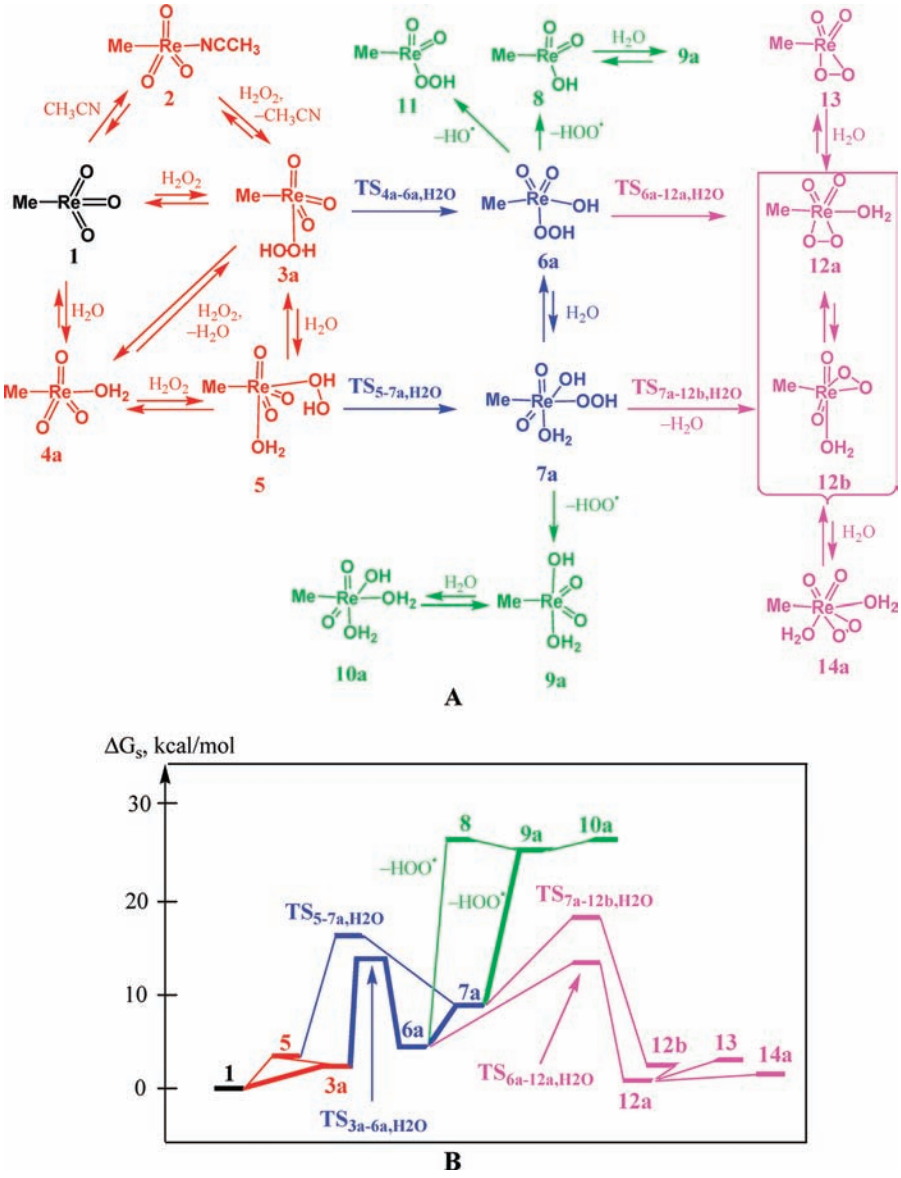

[a] Only the most important species are indicated. Color code: red, formation of initial adducts; blue, first H-transfer; green, formation of radicals and transformations of Re^{VI} species; magenta, second H-transfer and transformations of the formed species. Route 7 (the most favorable one) is marked by bold lines.

kcal/mol). In contrast, $\Delta H_{s,ap}$ of formation of the water complex **9** + HOO• is only 19.4 kcal/mol (consistent with the experiment values for the V systems), demonstrating the important role of an additional water molecule in the reaction mechanism. Consideration of the entropic factors indicates that both ΔG_s values—apparent and that for the S_N1 reaction—are also lower for the **9** + HOO• formation than for the **8** + HOO• formation. It is worthwhile to mention that the elimination of the HO• radical at this stage, i.e., from **6** leading to [$MeReO_2$(OOH)] **11**, requires 54.7 kcal/mol and, hence, should be ruled out. The apparent ΔG_s value for the generation of the HOO• radical from acetonitrile adducts [$MeReO_2$(OH)(OOH)(CH_3CN)] (**7a′**) is noticeably higher, by 5.2 kcal/mol, than that from the corresponding aquo complex [$MeReO_2$(OH)(OOH)(H_2O)] (**7a**). Hence, in this work, plausible pathways involving acetonitrile complexes are not considered.

In summary, the most favorable route for the formation of HOO• radicals within the general mechanism based on MTO includes the sequence of transformations (eq 7)

$$\mathbf{1} + H_2O_2 \rightarrow \mathbf{3a} \rightarrow \mathbf{6a} \rightarrow \mathbf{7a} \rightarrow \mathbf{9a} + HOO^{\bullet} \qquad (7)$$

This conclusion is based on the following arguments: (i) the 5-coordinate adduct [$MeReO_3$(HOOH)] **3a** is more stable (by 1.1 kcal/mol) than the 6-coordinate complex **5**; (ii) the activation barrier for the reaction **3a** → [$MeReO_2$(OH)(OOH)] (**6a**) is lower (by 2.2 kcal/mol) than for the reaction **5** → [$MeReO_2$(OH)(OOH)(H_2O)] (**7a**); (iii) complex **6a** is by 4.1 kcal/mol more stable than **7a**; however, (iv) despite this, the direct generation of the HOO• radicals from **6a** (**6a** → **8** + HOO•) requires slightly more energy (by 1.6 kcal/mol) than through the formation of complex **7a** {**6a** → **7a** → [$MeReO_2$(OH)(H_2O)] (**9a**) + HOO•}. Thus, up to the stage of formation of the hydroxo−hydroperoxo complexes,

Table 1. Energetic Characteristics (in kcal/mol) of the Reactions Discussed in the Text[a]

N	reaction	ΔH_s	ΔG_s	*N*	reaction	ΔH_s	ΔG_s
			Mechanisms Based on [$MeReO_3$]				
1	**1** + CH_3CN = **2**	−0.7	+3.7	7	**6a** → **8** + HOO•	31.8	21.9
2	**1** + H_2O_2 = **3a**	−5.0	+2.5	8	**7a** → **9a** + HOO•	25.9	16.2
3	**1**+ H_2O = **4a**	−6.9	−0.5	9	**6a** → **11** + HO•	63.5	54.7
4	**1** + H_2O + H_2O_2 → **5**	−9.7	+3.6	10	**1** + H_2O_2 → **8** + HOO•	28.1	26.9
5	**3a** → $\mathbf{TS_{3a-6a}}$	20.9	21.8	11	**1** + H_2O_2 + H_2O → **9a** + HOO•	19.4	25.3
5	**3a** → $\mathbf{TS_{3a-6a,H_2O}}$	2.5	11.6	12	**6a** → $\mathbf{TS_{6a-12a}}$	15.7	16.6
		6.8[b]	15.9	12	**6a** → $\mathbf{TS_{6a-12a,H_2O}}$	0.4	8.2
5	**3a** → **6a**	1.3	2.5	12	**6a** → **12a**	−4.0	−4.8
		0.2[b]	1.4[b]	13	**7a** → $\mathbf{TS_{7a-12b,H_2O}}$	1.6	10.0
6	**5** → $\mathbf{TS_{5-7a}}$	23.8	25.2	13	**7a** → **12b** + H_2O	0.6	−7.1
6	**5** → $\mathbf{TS_{5-7a,H_2O}}$	2.7	13.8	14	**12b** → **12a**	−1.8	−1.8
		8.8[b]	19.9	15	**12a** → **13** + H_2O	8.8	2.1
6	**5** → **7a**	3.2	5.5	16	**12a** + H_2O → **14a**	−4.7	1.3
		2.3[b]	4.6[b]				
			Mechanisms Based on Monoperoxo Complexes				
17	**12a** + H_2O_2 → **15a** + H_2O	3.9	4.8	26	**17a** → **21** + HOO•	25.2	15.4
18	**15a** → **15b**	0.6	0.8	27	**18a** → **22** + HOO•	23.4	13.7
19	**12a** + H_2O_2 → **16a**	−3.1	+4.0	28	**19b** → **23a** + HOO•	19.2	7.9
20	**15b** → $\mathbf{TS_{15b-17c,H_2O}}$	−0.9	+8.0	29	**20c** → **25a** + HOO•	24.0	13.3
20	**15b** → **17c**	10.9	11.2	30	**1** + 2H_2O_2 → **21** + H_2O + HOO•	28.2	27.5
21	**17c** → **17a**	−4.6	−4.9	31	**1** + 2H_2O_2 → **22** + H_2O + HOO•	28.0	27.9
22	**15b** → $\mathbf{TS_{15b-18d,H_2O}}$	2.1	11.2	32	**1** + 2H_2O_2 → **23a** + HOO•	17.7	23.5
22	**15b** → **18d**	13.2	14.3	33	**1** + 2H_2O_2 → **25a** + HOO•	20.0	26.6
23	**18d** → **18a**	−5.4	−5.8	34	**18a** → $\mathbf{TS_{18a-28a,H_2O}}$	−7.0	+1.7
24	**16a** → $\mathbf{TS_{16a-19b,H_2O}}$	−0.2	+9.2	34	**18a** → **28a**	−12.1	−12.0
24	**16a** → **19b**	9.4	11.5	35	**20c** → $\mathbf{TS_{20c-29a,H_2O}}$	−4.3	+3.0
25	**16a** → $\mathbf{TS_{16a-20c,H_2O}}$	1.6	11.1	35	**20c** → **29a**	4.1	1.8
25	**16a** → **20c**	6.9	9.2	36	**28a** → **27** + H_2O	13.7	6.3
			Mechanisms Based on Biperoxo Complexes and Regeneration of the Catalyst				
37	**27** + H_2O_2 → **30a**	−9.2	−0.7	49	**31b2** → $\mathbf{TS_{31b2-35a,H_2O}}$	−3.7	+6.2
38	**27** + H_2O_2 → **30b**	−0.9	+5.6	49	**31b2** → **35a**	−6.5	−4.1
39	**28a** + H_2O_2 → **31a**	2.0	7.5	50	**33a** → **37** + HOO•	26.2	15.5
40	**28a** + H_2O_2 → **31b1**	16.4	22.5	51	**32a** → **36** + HOO•	21.1	11.4
41	**28a** + H_2O_2 → **31b2**	18.0	25.5	52	**34a** → **38a** + HOO•	24.9	14.0
42	**29a** + H_2O_2 → **31a** + H_2O	−5.6	−5.3	53	**35a** → **40a** + HOO•	21.3	9.7
43	**30a** → $\mathbf{TS_{30a-32a,H2O}}$	1.9	10.3	54	**1** + 3H_2O_2 → **37** + 2H_2O + HOO•	43.3	44.0
43	**30a** → **32a**	10.9	10.4	55	**1** + 3H_2O_2 → **36** + 2H_2O + HOO•	29.1	29.6
44	**30b** → $\mathbf{TS_{30b-33e,H2O}}$	16.0	26.0	56	**1** + 3H_2O_2 → **38a** + H_2O + HOO•	18.9	26.6
44	**30b** → **33e**	22.4	25.1	57	**1** + 3H_2O_2 → **40a** + H_2O + HOO•	25.4	33.4
45	**27** + H_2O_2 → **27**•H_2O_2	0.6	6.6	58	**23a** + H_2O_2 → **42a** + H_2O	3.9	5.4
46	**27**•H_2O_2 → $\mathbf{TS_{27\bullet H_2O_2-33b,H2O}}$	0.8	11.5	59	**42a** → $\mathbf{TS_{42a-43a,H_2O}}$	−4.7	3.8
46	**27**•H_2O_2 → **33b**	11.9	14.8	59	**42a** → **43a**	−9.3	−7.8
47	**33b** → **33a**	−1.5	−1.6	60	**43a** → $\mathbf{TS_{43a-6a}}$	8.1	8.4
48	**31b1** → $\mathbf{TS_{31b1-34a,H_2O}}$	−10.0	+1.3	60	**43a** → **6a** + HO•	0.9	−5.6
48	**31b1** → **34a**	−15.0	−12.3				

[a] ΔH_s and ΔG_s values given for CH_3CN as solvent, unless stated otherwise. [b] Values given for H_2O as solvent.

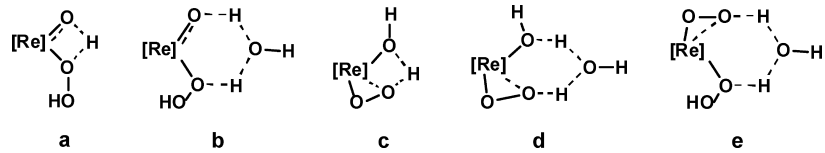

Figure 1. TSs for H-transfer from coordinated H_2O_2 to an oxo ligand (a, b) or to a peroxo ligand (e), or from coordinated hydroperoxo to an hydroxo ligand (c, d). Those with six-membered metallacycles bearing H_2O provide the most favorable H-transfers (water-assisted).

the route based on penta-coordinate species is more plausible than that involving the hexa-coordinate complexes, and this is determined by entropic factors. The generation of HOO• radicals at the last stage is more favorable from the hexa-coordinate complex **7a**, mostly due to the lower V−OOH bond energy in **7a** compared to **6a**.

(iv) Formation of Monoperoxo−Re Complexes. Complex **6a** can convert into the monoperoxo species [$MeReO_2$(OO)(H_2O)] (**12**) [to the most stable isomer **12a**, Schemes 3 and 1S (Supporting Information)] via an H-transfer from the OOH to the OH ligand with formation of a water molecule. Similarly to the previous step, the direct transfer via a four-membered cyclic TS ($\mathbf{TS_{6a-12a}}$) (Figure 1c) is rather energetically demanding ($\Delta G_s^{\ddagger}$ = 16.6 kcal/mol). However, the water-assisted reaction via $\mathbf{TS_{6a-12a,H_2O}}$, a six-membered metallacycle (Figure 1d), is characterized by a much lower $\Delta G_s^{\ddagger}$ value of 8.2 kcal/mol. The resulting complex **12a** may give [$MeReO_2$(OO)] (**13**) upon liberation

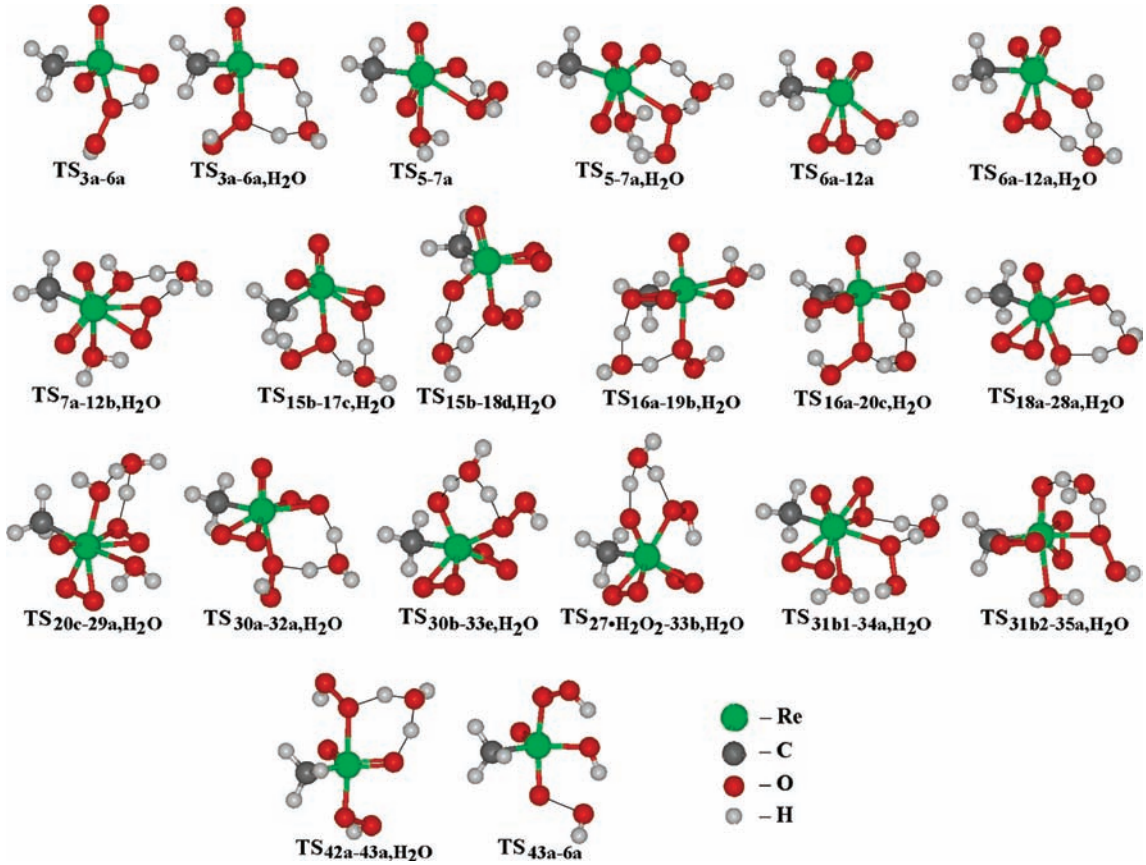

Figure 2. Equilibrium geometries of transition states discussed in the text.

of water. H-transfer from the OH ligand to the oxygen of the OOH ligand was not considered, because it is "forbiddingly slow".[35]

For the water-assisted H-transfer in complex **7a**, the low-energy six-membered (type d) transition state $\mathbf{TS_{7a-12b,H_2O}}$ was also located.[49] However, the search of the PES indicated that the product of this reaction is **12b** [the second most stable isomer of **12**, Schemes 3 and 1S (Supporting Information)] instead of the diaquo complex [MeReO$_2$(OO)(H$_2$O)$_2$] (**14**). Thus, species **14** may be formed upon addition of H$_2$O to **12** rather than directly from **7**.

2. Mechanisms Based on the Monoperoxo−Re Complexes. (i) Hydrogen Peroxide Adducts. Processes similar to those examined in the previous section for MTO may also take place when starting from the monopreoxo species **12**−**14** [Schemes 4 and 2S (Supporting Information), Table 1]. The first step is the formation of the adducts with hydrogen peroxide [MeReO$_2$(OO)(H$_2$O$_2$)] (**15**) and [MeReO$_2$(OO)(H$_2$O$_2$)(H$_2$O)] (**16**), e.g., upon slightly endoergonic substitution of H$_2$O for H$_2$O$_2$ in **12** or addition of H$_2$O$_2$ to **12**. For each of the complexes **15** and **16**, two stable isomers with small energy differences were found (**15a** and **15b**, **16a** and **16b**). In the most stable isomers **15a** and **16a**, the distances between the Re atom and the donor O-atom of H$_2$O$_2$ reach 2.68−2.77 Å. Despite this, the Re−O interaction should be considered a chemical bond, although weak, as suggested by the topological analysis of the electron density distribution. Indeed, the usage of the AIM method revealed the existence of a bond critical point for the Re−O$_{(H_2O_2)}$ interaction in both **15a** and **16a** species (see Figure 1S in Supporting Information).

(ii) Proton Migration. In this step, the hydrogen peroxide complex [MeReO$_2$(OO)(H$_2$O$_2$)] (**15**) undergoes an H-transfer either to a peroxo or to an oxo ligand, leading to [MeReO$_2$(OOH)$_2$] (**17**) or [MeReO(OO)(OH)(OOH)] (**18**), respectively [Schemes 4 and 2S (Supporting Information), Table 1]. For the migration to the peroxo ligand, the most favorable route starts from **15b** and includes the water-assisted H-transfer **15b** → **17c** (via $\mathbf{TS_{15b-17c,H_2O}}$ with the six-membered cycle e, Figure 1) and isomerization of **17c** to the most stable isomer **17a**. The $\Delta H_s^{\ddagger}$ value for the reaction **15b** → **17c** relative to the separate reactants **15b** and H$_2$O is negative and lower than the reaction enthalpy, ΔH_s. The reasons for such an effect for this and some other reactions are discussed in the Supporting Information. For the proton migration to the oxo ligand (**15** → **18** process), the most plausible route is also based on the **15b** isomer and consists in the **15b** → **18d** H-transfer followed by the isomerization to the most stable isomer (**18d** → **18a**).

Similar proton migrations from the ligated H$_2$O$_2$ to either a peroxo or an oxo ligand may also occur in the hexacoordinate complex [MeReO$_2$(OO)(H$_2$O$_2$)(H$_2$O)] (**16a**) [Schemes 4 and 2S (Supporting Information)]. The first

(49) Herein and in the further discussions we do not consider unimolecular H-transfers via four-membered transition states because, as it was indicated above, this would require significantly higher activation barriers.

Scheme 4. Mechanisms of HOO• Formation Based on Monoperoxo Complexes (A) and the Corresponding Energy Profile (B)[a]

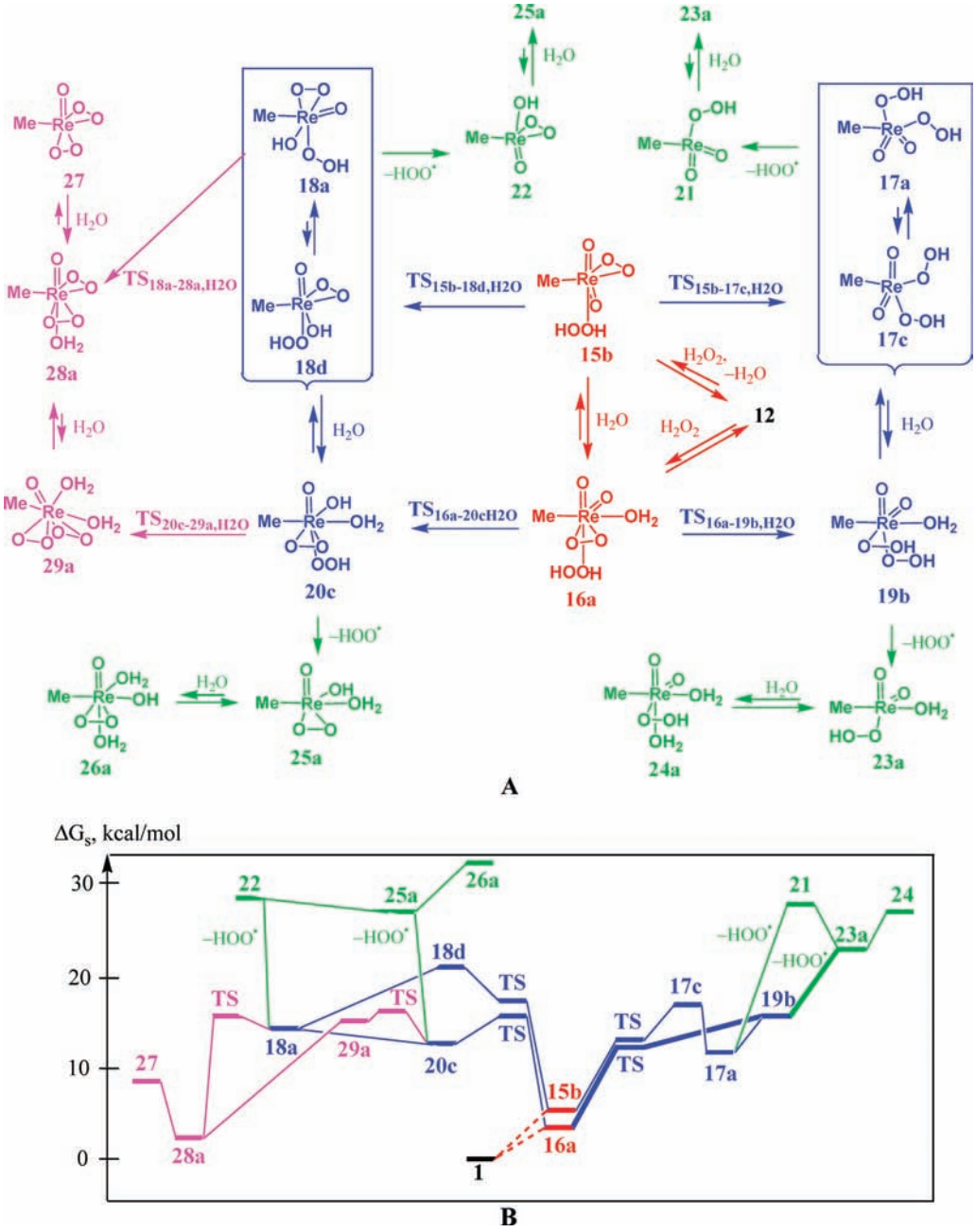

[a] Only the most important species are indicated; complete designations of TSs are not indicated for simplicity). For the color code, see Scheme 3. Route 10 (the most favorable one) is marked by bold lines.

process leads to the isomer **19b** of $[MeReO_2(OOH)_2(H_2O)]$, while the second reaction results in formation of the isomer **20c** of $[MeReO(OO)(OH)(OOH)(H_2O)]$. Both these routes proceed via six-membered transition states (types e or b, Figure 1) involving an additional water molecule ($\mathbf{TS_{16a-19b,H_2O}}$ and $\mathbf{TS_{16a-20c,H_2O}}$). Complexes **19** and **20** may also be formed upon addition of H_2O to **17** and **18**, respectively. Other less favorable routes for this general stage are discussed in the Supporting Information.

(iii) Radical Formation. Within the examined mechanism, the formation of the HOO• radicals may occur via dissociative S_N1 pathways **17** → $[MeReO_2(OOH)]$ (**21**) + HOO• and **18** → $[MeReO(OO)(OH)]$ (**22**) + HOO• (for penta-coordinate species) and **19** → $[MeReO_2(OOH)(H_2O)]$ (**23**) + HOO• and **20** → $[MeReO(OO)(OH)(H_2O)]$ (**25**) + HOO• (for hexa-coordinate species). No transition states corresponding to S_N2 one-step substitutions of HOO• for H_2O were found. The adiabatic M−OOH bond energies for **17a**, **18a**, **19b**, and **20c** (i.e., ΔG_s of S_N1 formation of HOO•) fall within the range of 7.9−15.4 kcal/mol and is minimal for **19b**, i.e. for the hexa-coordinate aquo−dihydroperoxo complex (Table 1).

In summary, an inspection of the energetic characteristics of the discussed processes allows us to conclude that among the four examined pathways of the HOO• radical formation (routes 8−11) based on the monoperoxo complexes, route 10 is the most favorable one, consisting of the sequence $[MeReO_2(OO)(H_2O_2)(H_2O)]$ (**16a**)

→ [MeReO$_2$(OOH)$_2$(H$_2$O)] (**19b**) → [MeReO$_2$(OOH)(H$_2$O)] (**23a**) + HOO$^\bullet$. Indeed, energetic demands for the formation of complexes **17a** (via **17c**), **19b**, and **20c** are similar, as seen from Scheme 4B, while formation of **18a** (via **18d**) requires ca. 5 kcal/mol more energy. However, the ΔG_s value of the last, rate-limiting step (formation of HOO$^\bullet$) for **19b** is significantly lower (by 5.4−7.5 kcal/mol) than for **17a**, **18a**, or **20c**. Furthermore, the *apparent* ΔG_s value of the formation of HOO$^\bullet$ along route 10 is also, by 4.4−3.1 kcal/mol, lower than for the other routes.

$$\mathbf{15b} \rightarrow \mathbf{17c} \rightarrow \mathbf{17a} \rightarrow \mathbf{21} + \mathrm{HOO}^\bullet \quad (8)$$

$$\mathbf{15b} \rightarrow \mathbf{18d} \rightarrow \mathbf{18a} \rightarrow \mathbf{22} + \mathrm{HOO}^\bullet \quad (9)$$

$$\mathbf{16a} \rightarrow \mathbf{19b} \rightarrow \mathbf{23a} + \mathrm{HOO}^\bullet \quad (10)$$

$$\mathbf{16a} \rightarrow \mathbf{20c} \rightarrow \mathbf{25a} + \mathrm{HOO}^\bullet \quad (11)$$

(iv) Formation of Diperoxo−Re Complexes. Complexes **18** and **20** may further convert, through H-transfer, to the diperoxo compounds [MeReO(OO)$_2$(H$_2$O)$_x$] [x = 0 (**27**), 1 (**28**), 2 (**29**)] [Schemes 4 and 2S (Supporting Information)]. The formation of **27** and **28** was previously confirmed both experimentally[35,45] and theoretically,[36a,b] and these complexes have been proposed to be the active species for a number of catalytic processes.[21] The structure of the most stable isomer of **28** (**28a**) corresponds to that found experimentally for this complex by X-ray analysis.[45a] The calculated bond lengths are in reasonable agreement with the experimental ones (the bond length deviations are within 0.04 Å) except for the Re−O$_{(H_2O)}$ bond, whose calculated value is longer, by 0.23 Å, than that obtained experimentally. According to Rösch et al.,[36a] this discrepancy can be accounted for by the influence of the cocrystallyzed diethyleneglycol dimethyl ether molecule in the compound studied experimentally.

The reactions **18a** → **28a** and **20c** → **29a** occur via transition states **TS$_{18a-28a,H_2O}$** and **TS$_{20c-29a,H_2O}$** (both of type d, Figure 1) with very small activation barriers. Complex **27** is formed from **28a** as a result of H$_2$O elimination.

3. Mechanisms Based on Diperoxo−Re Complexes. (i) Hydrogen Peroxide Adducts. The third main group of pathways affording HOO$^\bullet$ radicals is based on the diperoxo complexes **27**−**29**. This mechanism starts with the formation of the hydrogen peroxide adducts [MeReO(OO)$_2$(H$_2$O$_2$)] (**30**) and [MeReO(OO)$_2$(H$_2$O$_2$)(H$_2$O)] (**31**) [Schemes 5 and 3S (Supporting Information)] upon, for example, addition of H$_2$O$_2$ to **27** or **28** or upon the substitution of H$_2$O for H$_2$O$_2$ in **28** or **29**. For complexes **30** and **31**, two and three stable isomers were found, respectively, and, for the isomer **31b**, two forms with different orientations of H$_2$O$_2$ relative to the other ligands were calculated (**31b1** and **31b2**). The isomer **31c** is significantly less stable than **31a** and **31b** and therefore not involved in the mechanism. Although the AIM analysis indicates the presence of critical points for the Re−O$_{(H_2O_2)}$ bond in **30b** and the Re−O$_{(H_2O)}$ bond in **31a**, the very long metal−oxygen internuclear distances (3.09−3.20 Å) do not allow us to ascertain if the H$_2$O$_2$ and H$_2$O molecules belong to the inner or to the outer coordination sphere of the metal.

(ii) Proton Migration. The H-migration from the ligated H$_2$O$_2$ to a peroxo ligand in complex [MeReO(OO)$_2$(H$_2$O$_2$)] (**30**) takes place via a six-membered low-energy TS (**TS$_{30a-32a,H_2O}$**, of type e, Figure 1) corresponding to the reaction **30a** → [MeReO(OO)(OOH)$_2$] (**32a**). The direct H-transfer to the oxo ligand **30** → [MeRe(OO)$_2$(OH)(OOH)] (**33**) hardly occurs due to comparatively high activation barrier ($\Delta G_s^{\ddagger}$ = 26.0 kcal/mol for **TS$_{30b-33e,H_2O}$**). However, another more facile way to form **33** (i.e., **33b**) starting from [MeReO(OO)$_2$] (**27**) with an additional H$_2$O$_2$ molecule in the outer sphere (**27**·H$_2$O$_2$) rather than from **30** was found, thus omitting the stage of formation of an inner-sphere H$_2$O$_2$ adduct.

For the hexa-coordinate species, the proton transfer from the bound H$_2$O$_2$ to either a peroxo or an oxo ligand starts from **31b1** or **31b2**, respectively, and leads to [MeReO(OO)(OOH)$_2$(H$_2$O)] (**34a**) or [MeRe(OO)$_2$(OH)(OOH)(H$_2$O)] (**35a**) via **TS$_{31b1-34a,H_2O}$** or **TS$_{31b2-35a,H_2O}$**. The formation of **34a** is both kinetically and thermodynamically more favorable in comparison with **35a**. No TS for the channel from **31a** was located.

(iii) Radical Formation. The ΔG_s values of the S$_N$1 generation of HOO$^\bullet$ from **32a**−**35a** lie in the range of 9.7−15.5 kcal/mol (Table 1) (no TSs for S$_N$2 formation of HOO$^\bullet$ was found). Among the above-discussed pathways based on diperoxo complexes (routes 12−15), routes 13 and 15 involving the H-transfers to the oxo ligand should be excluded due to very high apparent ΔG_s of formation of HOO$^\bullet$ (44.0 and 33.4 kcal/mol). This situation is determined by the low stability of the hydroxo−diperoxo species [MeRe(OO)$_2$(OH)] (**37**) and [MeRe(OO)$_2$(OH)(H$_2$O)] (**40**). $\Delta G_{s,ap}$ of formation of HOO$^\bullet$ along route 12 is higher (by 3.0 kcal/mol) than for route 14. However, the latter includes a high-energy transition state for the **31b1** → **34a** step. A close examination of Scheme 5B reveals that the most favorable route 16 results from the combination of parts of routes 12 and 14, consisting in the sequence [MeReO(OO)$_2$(H$_2$O$_2$)] (**30a**) → [MeReO(OO)(OOH)$_2$] (**32a**) → [MeReO(OO)(OOH)$_2$(H$_2$O)] (**34a**) → [MeReO(OO)(OOH)(H$_2$O)] (**38a**) + HOO$^\bullet$.

$$\mathbf{30a} \rightarrow \mathbf{32a} \rightarrow \mathbf{36} + \mathrm{HOO}^\bullet \quad (12)$$

$$\mathbf{27}\cdot\mathrm{H_2O_2} \rightarrow \mathbf{33b} \rightarrow \mathbf{33a} \rightarrow \mathbf{37} + \mathrm{HOO}^\bullet \quad (13)$$

$$\mathbf{31b1} \rightarrow \mathbf{34a} \rightarrow \mathbf{38a} + \mathrm{HOO}^\bullet \quad (14)$$

$$\mathbf{31b2} \rightarrow \mathbf{35a} \rightarrow \mathbf{40a} + \mathrm{HOO}^\bullet \quad (15)$$

$$\mathbf{30a} \rightarrow \mathbf{32a} \rightarrow \mathbf{34a} \rightarrow \mathbf{38a} + \mathrm{HOO}^\bullet \quad (16)$$

Thus, for each of the general groups of the mechanism (i.e., based on MTO, mono- and diperoxo complexes), the most favorable route was selected (route 7, 10 or 16, respectively). Their comparison indicates that route 10 (involving monoperoxo species) is the most plausible one, since it has the lowest $\Delta H_{s,ap}$ and $\Delta G_{s,ap}$ values of HOO$^\bullet$ formation (17.7 and 23.5 kcal/mol, respectively) and these values correspond to the activation barrier of the overall process of radical formation in the system studied. The complete catalytic cycle for route 10 (including the formation

Scheme 5. Mechanisms of HOO• Formation Based on Diperoxo Complexes (**A**) and the Corresponding Energy Profile (**B**)[a]

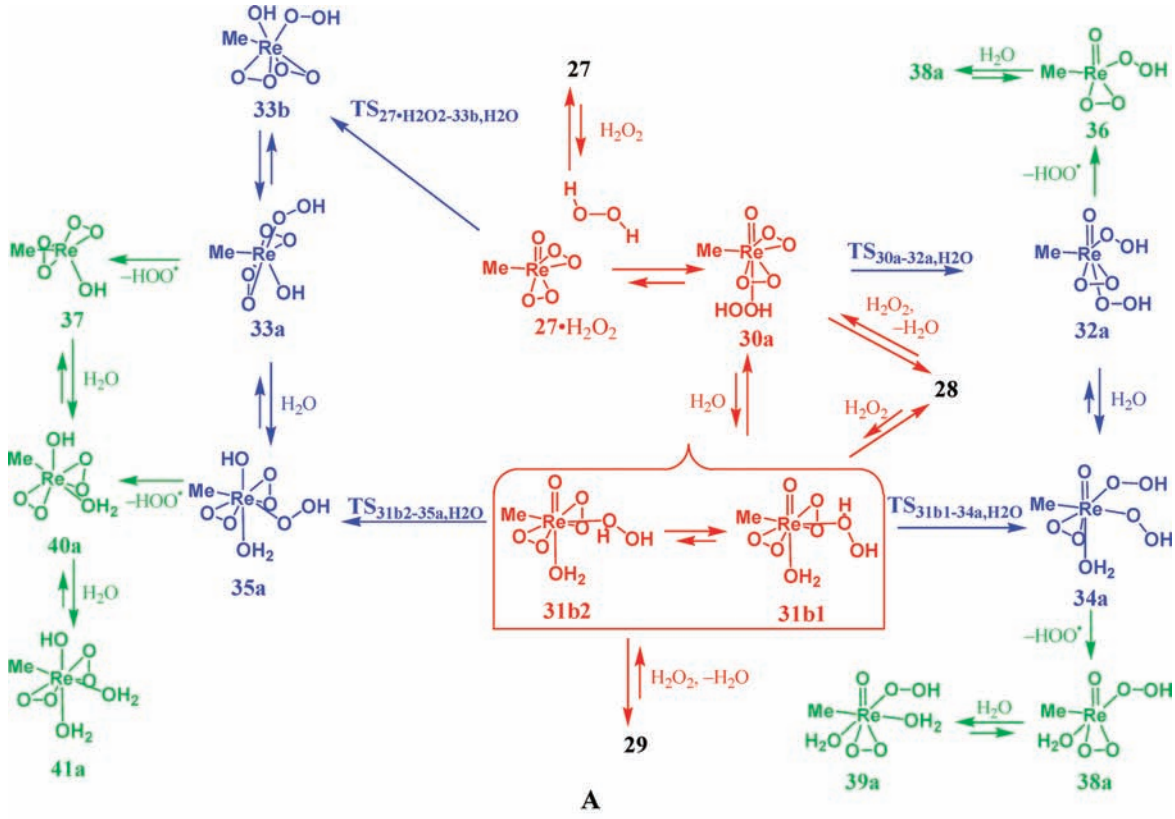

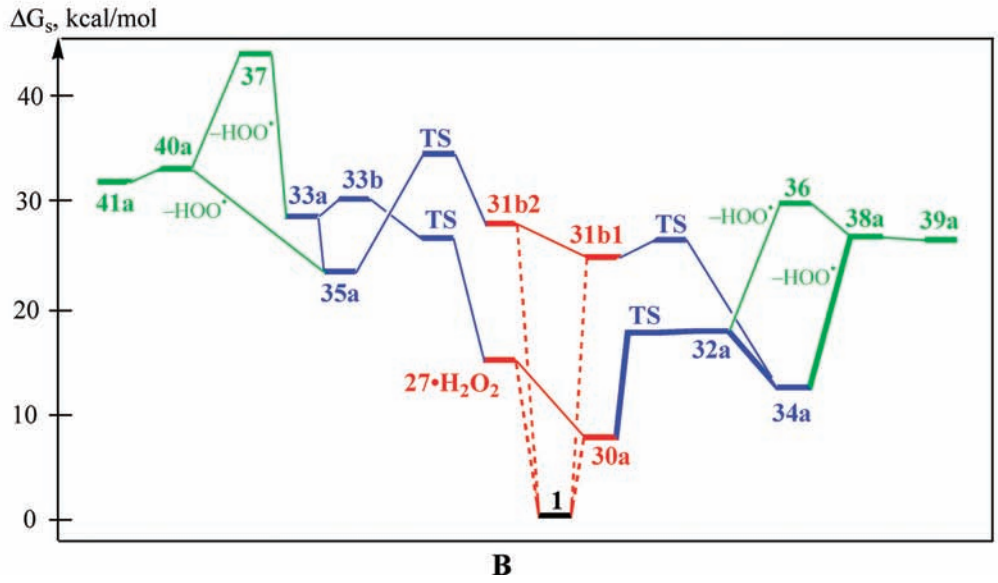

[a] Only the most important species are indicated; complete designations of TSs are not indicated for simplicity. For the color code see Scheme 3. Route 16 (the most favorable one) is marked by bold lines.

of the monoperoxo complex **16a** and the catalyst regeneration discussed below) is presented in Scheme 6.

4. Regeneration of the Catalyst and Formation of HO• Radicals. According to the mechanism proposed by Shul'pin et al.[9] (Scheme 1), the process following the homolytic dissociative liberation of the HOO• radical should proceed by reaction of the resulting reduced complex (in our case **8**−**10**, **21**−**26**, **36**−**41**) with H_2O_2 to form the HO• radical (which further reacts with the alkane) and to regenerate the catalyst. Here we examine this process only for one of those reduced Re^{VI} species, i.e. [Me-ReO_2(OOH)(H_2O)] (**23**) [Schemes 6, 7 and 4S (Supporting Information)], the complex formed in the most favorable route (10) (see above). The process starts with the formation of the hydrogen peroxide adduct [Me-ReO_2(OOH)(H_2O_2)] **42** (the most stable isomer **42a**) upon substitution of H_2O for H_2O_2 in **23** (the corresponding hexacoordinate intermediate resulting from the addition of H_2O_2 to **23** is not considered here). Then, water-assisted H-transfer within **42** from the coordinated H_2O_2 to an oxo ligand occurs

Scheme 6. The Most Favorable Catalytic Cycle for the Formation of Free HOO• and HO• Radicals

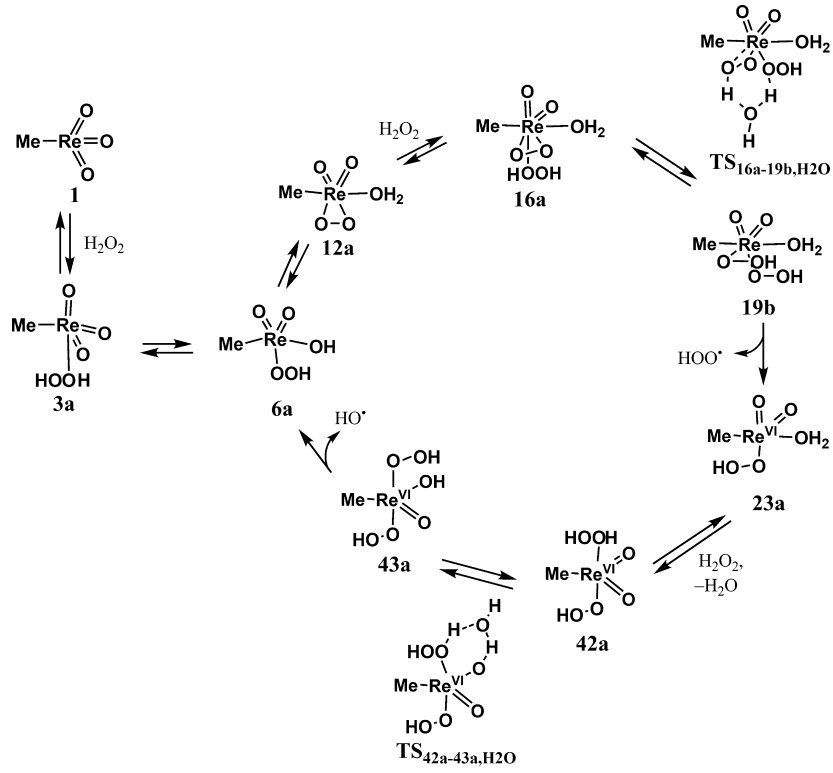

Scheme 7. Energy Profile for the Mechanism of HO• Formation and Regeneration of the Catalyst after the Liberation of the HOO• Radical (see also Scheme 6)[a]

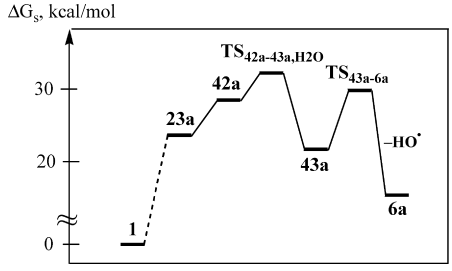

[a] Only the most important species are indicated.

via transition state $\mathbf{TS_{42a-43a,H_2O}}$ to give **43a**. Subsequent homolysis of the O−O(H) bond within one of the hydroperoxo ligands through $\mathbf{TS_{43a-6a}}$ requires an energy of only 8.4 kcal/mol (ΔG_s scale) (Table 1) and results in the generation of the HO• radical with concomitant formation of the Re^{VII} complex [MeReO$_2$(OH)(OOH)] **6a**, which starts a new cycle of the catalytic process.

Final Remarks

In accord with experimental observations,[20] the facile oxidation of some alkanes to alcohols and ketones catalyzed by MTO in the presence of H_2O_2 occurs via a free radical mechanism, and the rate-limiting step of such processes is the generation of free radicals.[9] In the present work, an extensive theoretical DFT study of plausible mechanisms of radical formation in the system [MeReO$_3$]/H_2O_2/H_2O−CH_3CN has been undertaken. The most favorable route (10) is based on the monoperoxo−Re^{VII} complex [MeReO$_2$(OO)(H_2O)] (**12**)—the species formed upon the reaction of MTO with H_2O_2—and includes the formation of an hydrogen peroxide adduct [MeReO$_2$(OO)(H_2O)(H_2O_2)] (**16**), H-transfer to a peroxo ligand, and S_N1-generation of the HOO• radical by homolytic cleavage of a Re^{VII}−OOH bond (Scheme 6). The reaction of the thus formed unsaturated and reduced Re^{VI} species [MeReO$_2$(OOH)(H_2O)] (**23a**) with H_2O_2 results, upon O−OH bond homolysis, in formation of the HO• radical (which reacts further with the alkane) with regeneration of an active oxidized Re^{VII}−oxo species (**6a**). Besides this route, other pathways based on MTO and diperoxo complexes (routes 7 and 16) also provide HOO• radicals, although with higher energy consumptions. The routes involving the H-transfer from a H_2O_2 ligand to a peroxo ligand are more effective in terms of HOO• formation than the pathways that include the H-transfer to an oxo ligand.

The present results corroborate the previous findings[9,19] that the direct H-transfers from a coordinated hydrogen peroxide within metal−oxo or metal−peroxo complexes are not kinetically favorable but should be assisted by an additional reagent. However, our calculations further show that the role of the H-transfer promotor can alternatively be played not by an additive or a particular *N*,*O*-ligand, but simply by water present in the reaction mixture, which stabilizes the corresponding transition state, forming a six-membered metallacycle, at least in the case of MTO. Another important role of the solvent is to provide the saturation of the metal coordination sphere, which decreases significantly the apparent activation energy of the radical formation, allowing the overall process to proceed easily at room temperature.

Although there are no experimental kinetic data on the oxidation of alkanes to alcohols and ketones catalyzed by MTO, some qualitative observations[20] suggest that the activation barriers should not deviate considerably upon the use of oxo−Re or oxo−V catalysts. Our computational results are consistent with this proposal, giving for the apparent activation enthalpy of $HOO^{\bullet}$ formation the value of 17.7 kcal/mol, while the corresponding experimental value[9] for the oxo−V-catalyzed process is 17 ± 2 kcal/mol. Thus, the overall type of mechanism originally proposed by Shul'pin et al. for oxo−vanadium complexes bearing *N*,*O*-ligands should also operate for oxo−Re catalysts such as MTO.

In the catalytic cycle, the peroxo complexes bear the metal in the highest oxidation state, i.e. Re^{VII} (d^0), but the [Re^{VII}−OOH] bond homolysis that generates the $HOO^{\bullet}$ radical forms a reduced Re^{VI} (d^1) species. Oxidation to Re^{VII} occurs at the stage of the homolytic O−O cleavage at the hydroperoxide ligand in [Re^{VI}]−O−OH to give the $HO^{\bullet}$ radical with regeneration of an active [Re^{VII}]═O species. This Re^{VII}/Re^{VI} behavior relates to that of the V^{V}/V^{IV} system of Shul'pin and eventually can also be displayed by other catalysts in which the metal has two easily available oxidation states ($M^{n/n-1}$) of comparable stability, such as other high oxidation state group 5−7 metal oxides[20] and even some copper(II)[14,50] catalyst precursors, that we have found to be highly active in alkane peroxidative oxidation reactions, which also proceed via free radical mechanisms. We are currently investigating the generality of such hypotheses.

Acknowledgment. This work has been partially supported by the Fundação para a Ciência e a Tecnologia (FCT) and its POCI 2010 program (FEDER funded), Portugal. M.L.K. is grateful to the FCT for the fellowship (Grant BPD/34165/2006) and to the FCT and IST for a research contract within Ciência 2007 scientific programme.

Supporting Information Available: Additional discussion of activation energies and less favorable pathways; contour line diagrams of the Laplacian distribution and bond paths for some of the structures; complete schemes of the investigated mechanisms (including ball and stick format); tables with a general view of equilibrium geometries of all calculated structures, their total energies, enthalpies, entropies, and Gibbs free energies; and a complete table with energetic characteristics of all studied reactions. This material is available free of charge via the Internet at http://pubs.acs.org.

IC801753T

(50) (a) Nesterov, D. S.; Kokozay, V. N.; Dyakonenko, V. V.; Shishkin, O. V.; Jezierska, J.; Ozarowski, A.; Kirillov, A. M.; Kopylovich, M. N.; Pombeiro, A. J. L. *Chem. Commun.* **2006**, 4605. (b) Di Nicola, C.; Karabach, Y. Y.; Kirillov, A. M.; Monari, M.; Pandolfo, L.; Pettinari, C.; Pombeiro, A. J. L. *Inorg. Chem.* **2007**, *46*, 221.